Blood oxygenation-level dependent cerebrovascular reactivity imaging as strategy to monitor CSF-hemoglobin toxicity

Blood oxygenation-level dependent cerebrovascular reactivity imaging as strategy to monitor CSF-hemoglobin toxicity

Bart R. Thomson,[a,b] Henning Richter,[c,d] Kevin Akeret,[a] Raphael M. Buzzi,[b] Vania Anagnostakou,[e,f] Christiaan H.B. van Niftrik,[a] Nina Schwendinger,[a] Zsolt Kulcsar,[d,e] Peter W. Kronen,[d,g] Luca Regli,[a] Jorn Fierstra,[a] Dominik J. Schaer,[b] and Michael Hugelshofer,[a,d]

Objectives: Cell-free hemoglobin in the cerebrospinal fluid (CSF-Hb) may be one of the main drivers of secondary brain injury after aneurysmal subarachnoid hemorrhage (aSAH). Haptoglobin scavenging of CSF-Hb has been shown to mitigate cerebrovascular disruption. Using digital subtraction angiography (DSA) and blood oxygenation-level dependent cerebrovascular reactivity imaging (BOLD-CVR) the aim was to assess the acute toxic effect of CSF-Hb on cerebral blood flow and autoregulation, as well as to test the protective effects of haptoglobin. *Methods:* DSA imaging was performed in eight anesthetized and ventilated sheep (mean weight: 80.4 kg) at baseline, 15, 30, 45 and 60 minutes after infusion of hemoglobin (Hb) or co-infusion with haptoglobin (Hb:Haptoglobin) into the left lateral ventricle. Additionally, 10 ventilated sheep (mean weight: 79.8 kg) underwent BOLD-CVR imaging to assess the cerebrovascular reserve capacity. *Results:* DSA imaging did not show a difference in mean transit time or cerebral blood flow. Whole-brain BOLD-CVR compared to baseline decreased more in the Hb group after 15 minutes (Hb vs Hb:Haptoglobin: -0.03 ± 0.01 vs -0.01 ± 0.02) and remained diminished compared to Hb:Haptoglobin group after 30 minutes (Hb vs Hb:Haptoglobin: -0.03 ± 0.01 vs 0.0 ± 0.01), 45 minutes (Hb vs Hb:Haptoglobin: -0.03 ± 0.01 vs 0.01 ± 0.02) and 60 minutes (Hb vs Hb:Haptoglobin: -0.03 ± 0.02 vs 0.01 ± 0.01). *Conclusion:* It is demonstrated that CSF-Hb toxicity leads to rapid cerebrovascular reactivity impairment, which is blunted by haptoglobin co-infusion. BOLD-CVR may therefore be further evaluated as a monitoring strategy for CSF-Hb toxicity after aSAH.

Keywords: BOLD-CVR—Imaging—CSF-Hb—Early detection

Introduction

Aneurysmal subarachnoid hemorrhage (aSAH) is a severe form of intracranial bleeding caused by the rupture of an intracranial aneurysm,[1] which accounts for 5-10% of all strokes.[2] In addition to the early brain injury occurring within the first 72 hours after SAH,[3] patient outcome is mainly determined by secondary brain injury (SAH-SBI), which occurs between 3-14 days after the initial

From the [a]Department of Neurosurgery, Clinical Neuroscience Center, University Hospital and University of Zurich, Zurich, Switzerland; [b]Division of Internal Medicine, University Hospital of Zurich, Zurich, Switzerland; [c]Clinic for Diagnostic Imaging, Department of Clinical Diagnostics and Services, Vetsuisse Faculty, University of Zurich, Zurich, Switzerland; [d]Center for Applied Biotechnology and Molecular Medicine (CABMM), University of Zurich, Zurich, Switzerland; [e]Department of Neuroradiology, Clinical Neuroscience Center, University Hospital and University of Zurich, Zurich, Switzerland; [f]Department of Radiology, University of Massachusetts Medical School, Worcester, MA, USA; and [g]Veterinary Anaesthesia Services – International, Winterthur, Switzerland.

Received October 27, 2022; revision received December 27, 2022; accepted January 9, 2023.

Corresponding author. E-mail: michael.hugelshofer@usz.ch.

1052-3057/$ - see front matter

https://doi.org/10.1016/j.jstrokecerebrovasdis.2023.106985

bleeding.[4] Three main components of SAH-SBI are identified: 1. angiographic vasospasm in large cerebral arteries (aVSP); 2. radiologically diagnosed delayed cerebral ischemia; and 3. clinically evident delayed ischemic neurologic deficits. SAH-SBI is a complex process and recent evidence indicates that one of the main drivers may be the acute toxicity of cell-free hemoglobin in the cerebrospinal fluid (CSF-Hb).[5]

The pathophysiology is believed to involve the gradual lysis of erythrocytes in the subarachnoid space, thereby releasing large amounts of Hb,[5,6] causing direct oxidative tissue injury[7,8] and interaction with nitric oxide (NO) signaling in the arterial vessel wall, resulting in cerebrovascular disruption.[9,10] Recent findings from our group[10] and others[11] suggest that scavenging of CSF-Hb by haptoglobin mitigates these negative effects by preventing CSF-Hb tissue penetration, thus maintaining NO signaling. However, it remains unknown whether CSF-Hb toxicity induced cerebrovascular disruption primarily occurs on the level of major cerebral arteries or if toxic effects on microcirculation[11,12] significantly disturb the autoregulatory control of cerebral perfusion. To answer this question, a translational sheep model with direct intraventricular injection of cell-free Hb or co-infusion of Hb with haptoglobin was used to observe macrovascular effects using digital subtraction angiography (DSA).[13] Additionally, blood oxygenation-level dependent cerebrovascular reactivity (BOLD-CVR) imaging was performed to assess effects of CSF-Hb on the cerebrovascular autoregulatory reserve capacity on a microvascular level.[14,15] Imaging strategies, which allow for detection of acute CSF-Hb effects in aSAH patients may provide important guidance for clinical studies targeting these toxicity pathways.

Methods

General

This study was conducted according to the Swiss Animal Welfare Act (TschG, 2005) and the Swiss Animal Welfare Ordinance (TSchV, 2008) received ethical approval from the Swiss Federal Veterinary Office Zurich (animal license no. ZH 234/17). The authors complied with the ARRIVE guidelines. A total of 20 female Swiss alpine sheep, aged 2-4 years and obtained from the Staffelegghof (see supplemental material) were used during this study. Eight sheep were used during the DSA experiment (n= 4 Hb; n=4 Hb:Haptoglobin) and twelve during the BOLD-CVR experiment (n=6 Hb; n=6 Hb:Haptoglobin, Fig. 1B). Prior to the experiments the animals underwent a health check (clinical and blood examination) by a veterinarian and were randomly assigned to treatment groups. All involved personnel were blinded for group allocation until data analysis.

In both experiments, the order of substance infusion per animal was spread homogeneously to minimize potential confounding influences. In each experiment, the parameters of two scans prior to substance infusion were averaged and are presented as the baseline. In the BOLD-CVR experiment, two animals were excluded due to substance infusion failure and due to a physiologically impossible signal response in the baseline scans, identifying the baseline scans as corrupt. Under general anesthesia, surgical navigation was used to instrument the ventilated sheep with a left frontal external ventricular drain (EVD, DePuys Synthes). The model is further described in detail in the appendix. A PHD Ultra syringe pump (Harvard Apparatus) was connected to the EVD through which an excess (3 mL, 3 mmol/L) of Hb or Hb:Haptoglobin was infused within 6 minutes. In both experiments half of the group was infused with Hb, and the other half with Hb:Haptoglobin complex (Fig. 1D).

Hemoglobin and Hemoglobin-Haptoglobin complexes

Hb was purified from sheep blood as previously described.[16] Hb concentrations were determined by spectrophotometry as described and are given as molar concentrations of total heme (1M Hb tetramer is, therefore, equivalent to 4M heme).[9] For all Hb used in these studies, the fraction of ferrous oxyHb (HbFe2+O2) was always greater than 98% as determined by spectrophotometry. Haptoglobin from human plasma (phenotype 1-1) was obtained from CSL Behring.

DSA imaging

Allura Clarity angiography suite (Philips Healthcare, Best, The Netherlands) was used to perform DSA with an angiographic 5F catheter (Cordis) placed into the largest anastomotic branch of the right maxillary artery supplying the extradural rete mirabile and the internal carotid artery. Standardized pump injections of contrast media were performed to ensure comparability between pre- and post-substance infusion images. Prior to infusion of the respective substance, two DSA acquisitions were performed, followed by four acquisitions at respectively 15, 30, 45 and 60 minutes after the start of substance infusion.

DSA data processing

Prior to post-processing the whole cerebrum was segmented (Fig. 1C) in the 2D perfusion image. Sequentially, two parameters (Fig. 1A) were extracted and analyzed with a customized algorithm in Python. Mean transit time (MTT) was defined as the time from arrival of the contrast fluid till the center of mass of the density curve. Cerebral blood flow (CBF) was derived as cerebral blood volume (CBV) / MTT, where CBV is defined as the area under the contrast density curve.

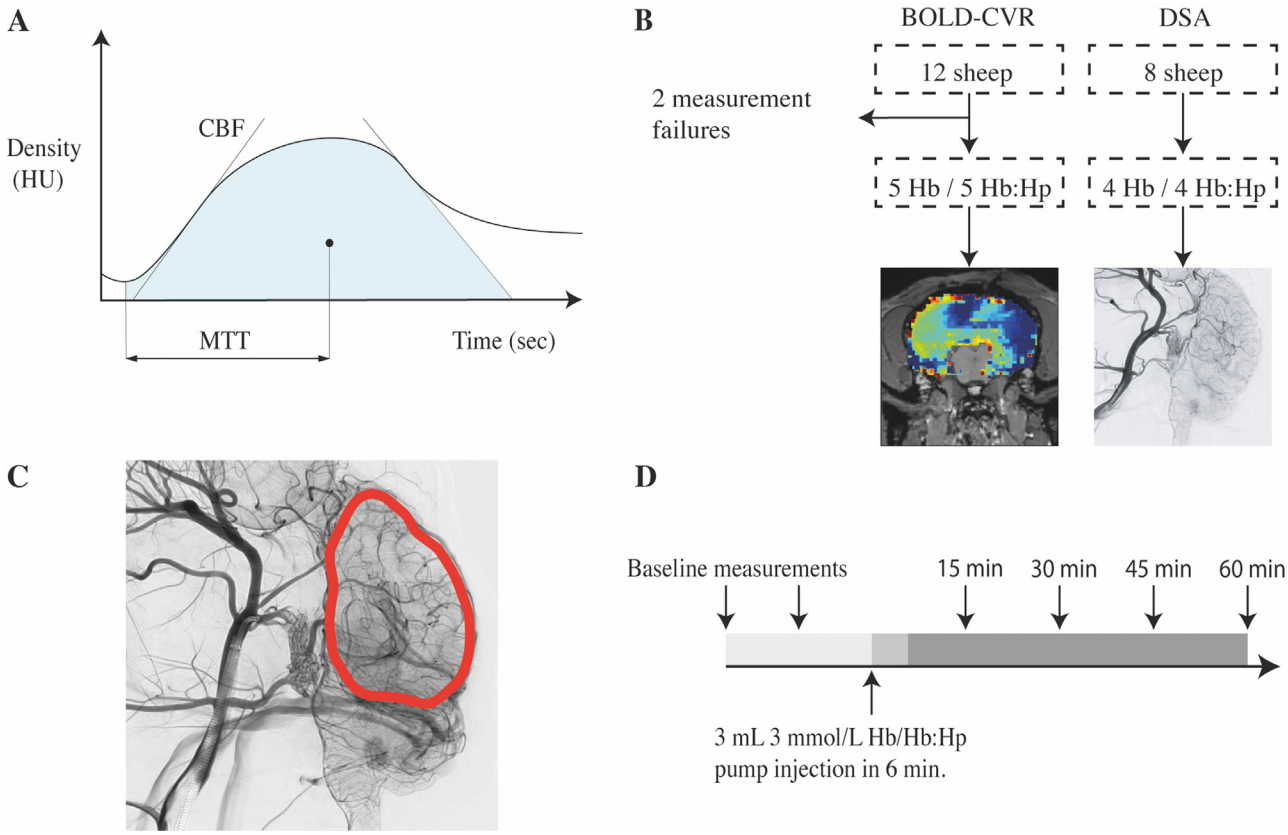

Fig. 1. ***Density curve analysis and DSA region of interest.*** *(**A**) DSA-derived flow parameters MTT and CBF (**B**) Illustration of the experimental workflow (**C**) Full brain region of interest (indicated in red) used for computation of DSA parameters (**D**) Scanning protocol, two baseline acquisitions prior to substance infusion, followed by four acquisitions post substance infusion.*

BOLD imaging

MR images were acquired on a 3 Tesla MR unit (Philips Ingenia) with a 32-channel head coil. The scanning protocol consisted of a T1-weighted sequence, two 2D EPI BOLD fMRI sequences, followed by a T2-weighted sequence during which infusion of the respective substance took place and ultimately four 2D EPI BOLD fMRI sequences at respectively 15, 30, 45 and 60 minutes after the onset of substance infusion. In one animal in the Hb: Haptoglobin group, scan acquisition at the 60 minutes time point could not be completed due to time constraints. In all acquisitions whole-brain volumes were acquired with a 2 × 2 × 2 mm3 voxel size. Additional fMRI parameters were an acquisition matrix of 112 × 112 × 33 slices with ascending interleaved acquisition without slice gap, repetition time (TR)/ echo time (TE) 1896/17 ms, a 75-degree flip angle with a bandwidth of 1900 Hz/Px. During acquisition PetCO2 was maintained for 120 s at normocapnia, followed by an abrupt hypercapnic step increase of 15 mmHg for 240 s, before returning to normocapnia for 360 s. Normocapnia depended on the resting PetCO2 of the individual animal, as these were found to range in between individual sheep. The hypercapnic step was achieved by an automated gas blender that adjusts the gas flow and composition to a sequential gas delivery breathing circuit (RepirAct, Thornhill Research Institute, Toronto, Canada) to control the end-tidal partial pressures of PetCO2 and oxygen (PetO2), as described in.[15,17]

BOLD-CVR data processing

All acquired imaging was preprocessed using Statistical Parametric Mapping 12 (SPM 12, Wellcome Trust Centre for Neuroimaging, Institute of Neurology, University College London, UK). All temporal BOLD volumes were realigned to the mean of their series, followed by a registration of the anatomical volumes to the same mean image. Ultimately, the functional images were smoothed with a Gaussian kernel of 8mm full width at half maximum. Consecutively, the anatomical acquisitions were used to manually delineate the cerebrum, using 3DSlicer 4.11.0.[18]

Further temporal processing was performed in Python, where linear detrending of the data was followed by, like,[19] a low band-pass filter with a filter cut-off of 0.125 Hz and lowess smoothing[20] using 16 dynamics (6%). Ultimately, the PetCO2 course was resampled to match the TR of the BOLD data. CVR calculations were

performed after conclusion of the experiments based on a standardized method presented by van Nifrik et al.[21]

Results

In the DSA experiment, MTT increases slightly in both groups (Fig. 2A & 2B), and CBF (in mL/100g/min) shows a slight decrease (Fig. 2C & 2D). However, no apparent differences are observed between the groups following their respective injection. When imaged with BOLD-fMRI, all animals injected with Hb demonstrate a decline in CVR as early as 15 minutes post infusion, after which it stabilizes on this reduced level (Fig. 2E and 2F). In contrast, the Hb:Haptoglobin group demonstrates an increase in CVR. The numerical values of the comparative data between the different modalities are presented in Table 1 and Table 2. Fig. 3 presents the decrease in CVR with respect to the baseline following Hb infusion, whereas an increase in CVR is observed after injection of Hb:Haptoglobin. Here, the overall decrease in CVR appears more apparent in cortical regions in proximity of the CSF space, however, no clear difference could be quantified between gray and white matter.

Discussion

Our study demonstrates that BOLD-CVR imaging is able to detect early-onset toxicity of CSF-Hb, which can be prevented by haptoglobin co-infusion. Contrarily, the functional DSA derived parameters MTT and CBF were not sensitive enough to detect the difference between Hb or Hb:Haptoglobin infusion. These findings strengthen the rationale for BOLD-CVR monitoring as a strategy to detect CSF-Hb toxicity and haptoglobin treatment effects after aSAH.

In our model, CSF-Hb induced CVR impairment can be detected as early as 15 minutes after Hb infusion into the CSF and therefore precedes Hb-induced macrovascular constriction observed in previous studies.[10] The decreased cerebrovascular response lasts up to 1 hour after infusion of Hb, when compared to baseline CVR. Interestingly, after co-infusion of Hb with haptoglobin we found an increase of CVR over time, when compared to baseline. Upon qualitative assessment these protective effects seem larger in the cortical regions in proximity to the subarachnoid space. Physiologically this could be explained by the cortico-ventricular direction of CSF flow along the perivascular spaces, diluting Hb with highest concentrations found in juxtacortical regions.[22]

In contrast to BOLD-CVR, the DSA derived parameters MTT and CBF were not sensitive enough to detect variations between Hb or Hb:Haptoglobin infusion. These differences are explained by the functional microvascular changes that are better reflected by BOLD-CVR versus the macrovascular changes detectable by DSA. This could partially explain the clinical observation of occurrence of SAH-SBI in absence of angiographic vasospasm,[23] and presence of vasospasm when SAH-SBI is absent.[24] A previous clinical study[5] showed strong evidence for a positive association between the occurrence of SAH-SBI and daily measured CSF-Hb concentrations. Future research should be scoped towards relating quantitative BOLD-CVR measurements in aSAH patients to CSF-Hb concentration and the clinical presentation of SAH-SBI. In this regard, the BOLD-CVR results that we present, suggest a possible role for BOLD-CVR as a powerful clinical imaging strategy to guide therapeutic interventions to prevent CSF-Hb toxicity in the brain.

Due to the autoregulatory efficiency that is reflected by BOLD-CVR, we argue that already after 15 minutes, CSF-Hb affects CBF on a microvascular level. From our experiments it remains unknown whether the protective myogenic mechanism of autoregulation itself is affected, or whether the reduction in CVR reflects a reduced efficiency of autoregulatory control. Other groups have suggested that there is a link between impaired CVR and the risk of ischemic events.[25-27] Additionally, in SAH patients it was shown that a decrease in CVR was independently associated with the occurrence of DCI.[28] Moreover, impaired CVR is likely to precede reduction of regional CBF in brain tissue at risk for DCI. Hence, on a functional level the observed effect of unbound CSF-Hb might contribute to the occurrence of delayed cerebral ischemia and delayed ischemic neurologic deficits following aSAH. Moreover, haptoglobin co-infusion seems to prevent these microvascular changes. These findings further support the therapeutic concept of intracerebroventricular haptoglobin administration as strategy to target CSF-Hb toxicity after aSAH,[5] which is planned to be translated into clinical studies in the near future.

The sensitivity of BOLD-CVR imaging to detect CSF-Hb effects on cerebral blood flow regulation may be of high relevance in a clinical context. Since it appears that the BOLD-CVR signal changes forego the manifestation of delayed cerebral ischemia or delayed ischemic neurologic deficits, early detection of CSF-Hb toxicity may allow for targeted therapeutic interventions with the aim to improve microvascular function and perfusion. Consequently, the demonstrated sensitivity of BOLD-CVR harbors the potential to lower morbidity and mortality associated with SAH-SBI.

Our study contains several limitations. Firstly, our model was designed to show the temporospatial vascular effects of CSF-Hb on CBF regulation. BOLD-CVR is assumed to be a surrogate marker for CBF based on the strong correlation between CBF measured by arterial spin labeling and the BOLD signal.[29] However, the BOLD signal has a complex dependency upon hematocrit, cerebral blood volume and cerebral metabolic rate and is not only dependent on cerebral blood flow.[30] Our experimental setup did not allow for appropriate anatomical quantification of Hb-induced macrovascular constrictions in the BOLD-CVR experiments. The absence of simultaneous

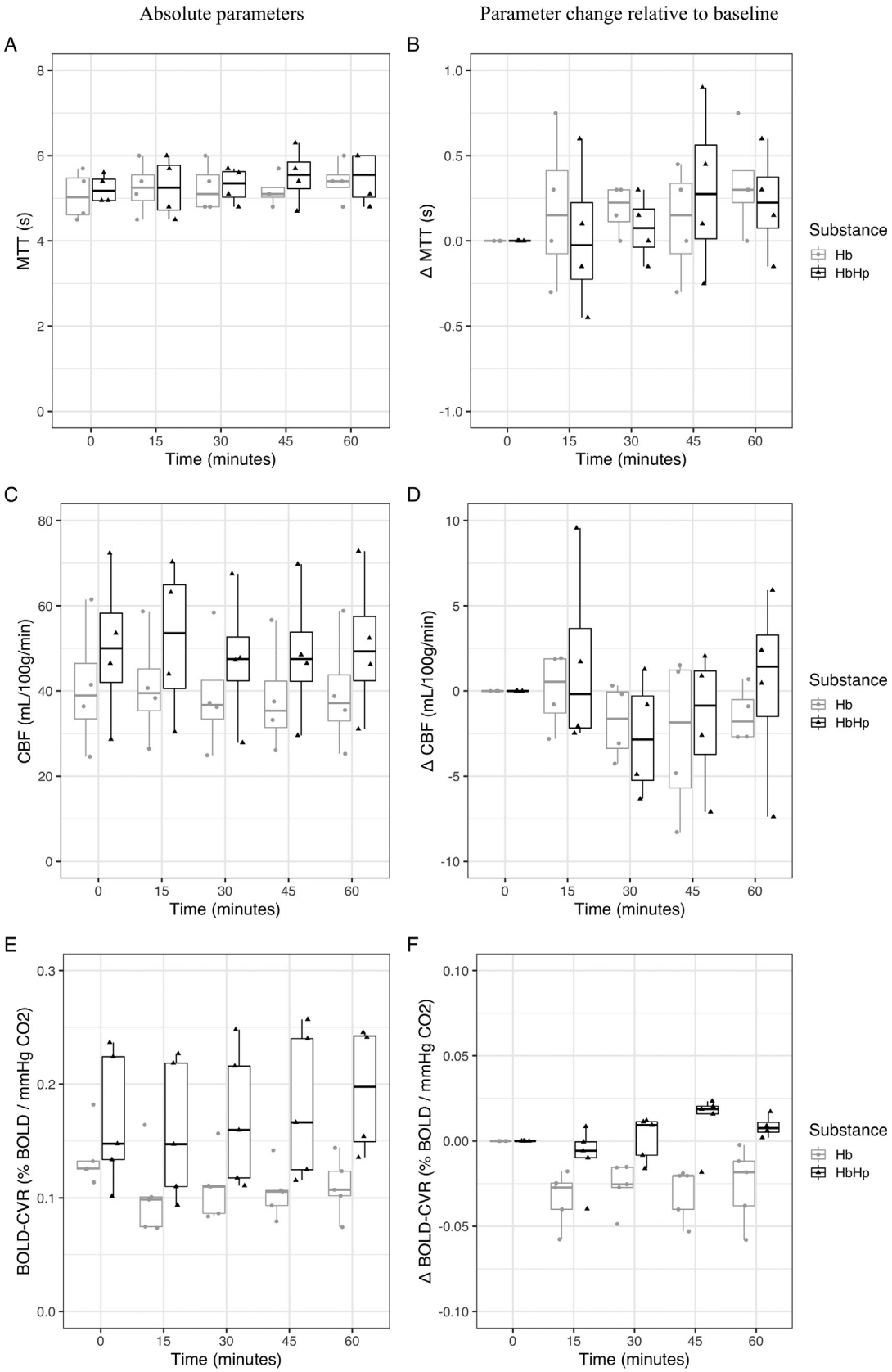

Fig. 2. ***Temporal dynamics of cerebrovascular parameters after intracerebroventricular Hb or Hb:Haptoglobin.*** *Absolute temporal profiles of DSA derived parameters (**A**) MTT, (**C**) CBF and (**E**) BOLD-CVR. Changes with respect to baseline of DSA derived parameters (**B**) MTT, (**D**) CBF and (**F**) BOLD-CVR. Hb is indicated in gray and Hb:Haptoglobin (Hb:Hp) in black. All boxplots present the 25% and 75% IQR around the median, with the whiskers extending to maximally 1.5 * IQR, indicating potential outliers.*

Table 1. *Absolute temporal dynamics of cerebrovascular parameters after intracerebroventricular Hb or Hb:Haptoglobin injection.*

	MTT		CBF		CVR	
	Hb	Hb:Hp	Hb	Hb:Hp	Hb	Hb:Hp
Unit	seconds		mL/100g/min		% BOLD/mmHg CO2	
Baseline	5.06 ± 0.50	5.25 ± 0.32	40.99 ± 13.33	50.26 ± 15.65	0.14 ± 0.02	0.17 ± 0.05
15 min	5.25 ± 0.54	5.25 ± 0.62	41.04 ± 11.53	51.95 ± 15.73	0.10 ± 0.03	0.16 ± 0.05
30 min	5.25 ± 0.50	5.32 ± 0.39	39.19 ± 12.12	47.58 ± 14.01	0.11 ± 0.03	0.17 ± 0.05
45 min	5.18 ± 0.33	5.55 ± 0.54	38.37 ± 11.33	48.58 ± 14.28	0.11 ± 0.02	0.18 ± 0.06
60 min	5.40 ± 0.42	5.48 ± 0.54	39.59 ± 12.17	50.62 ± 14.98	0.11 ± 0.02	0.19 ± 0.05

Table 2. *Temporal dynamics of cerebrovascular parameters after intracerebroventricular Hb or Hb:Haptoglobin, relative to the baseline values prior to substance injection.*

	MTT		CBF		CVR	
	Hb	Hb:Hp	Hb	Hb:Hp	Hb	Hb:Hp
Unit	seconds		mL/100g/min		% BOLD/mmHg CO2	
Baseline	0.0	0.0	0.0	0.0	0.0	0.0
15 min	0.19 ± 0.39	-0.0 ± 0.38	0.05 ± 1.98	1.68 ± 4.83	-0.03 ± 0.01	-0.01 ± 0.02
30 min	0.19 ± 0.12	0.08 ± 0.17	-1.8 ± 1.93	-2.69 ± 3.05	-0.03 ± 0.01	0.0 ± 0.01
45 min	0.11 ± 0.29	0.3 ± 0.41	-2.62 ± 4.12	-1.69 ± 3.56	-0.03 ± 0.01	0.01 ± 0.02
60 min	0.34 ± 0.27	0.22 ± 0.27	-1.4 ± 1.41	0.35 ± 4.87	-0.03 ± 0.02	0.01 ± 0.01

anatomical imaging makes it impossible to directly quantify the physiological contribution of macrovasospasm to the decrease in CVR. However, the absence of macrovascular changes in the DSA group hint towards absence of a macrovascular contribution in the reduction of CVR. Secondly, baseline CVR differences are present between the Hb and Hb:Haptoglobin group, which is most likely due to the small sample size, however, still within a range observed within healthy human subjects.[31] This small sample size limited quantitative statistical testing. However, as the clinically relevant differences in CVR were expected to be small, a sample size with adequate power for statistical analysis in these large animal experiments has been judged inappropriate due to animal welfare considerations. Lastly, a sheep model was chosen due to the similar cortical architecture and size when compared to humans,[32] allowing for adequate imaging. To realize a stable model, anesthesia was maintained with isoflurane, which in itself does not affect CSF production, however dosage has been shown to change CSF reabsorption[33] and affect CBF, resulting in CVR blunting.[34] However, due to the constant isoflurane administration during the individual experiments, we did not expect a relevant temporal effect on our readouts and the conditions in our experiments were reproducible and comparable between groups.

Conclusions

We have demonstrated that BOLD-CVR is able to quantify microvascular effects of CSF-Hb, prior to macrovascular constriction. This sensitivity allows for earlier adaptive measures and guide therapeutic interventions such as scavenging of CSF-Hb with intracerebroventricular application of haptoglobin. Contrarily, the DSA derived parameters MTT and CBF were not sensitive enough to discriminate between Hb and Hb:Haptoglobin co-infusion. Our results contribute to establishing BOLD-CVR as an imaging modality to detect vascular changes after aSAH with a high sensitivity and strengthen the rationale for novel treatment strategies targeting Hb-toxicity after aSAH.

Consent for publication

All authors have read and approved the submitted manuscript.

Availability of supporting data

Data and code can be made available upon reasonable request via author correspondence.

Declaration of Competing Interest

MH and DJS are inventors on a patent application on the use of haptoglobin in aneurysmal subarachnoid hemorrhage (WO2020/234195). MH, DJS, RMB, and KA are inventors on a patent application on the use of hemopexin and haptoglobin in aneurysmal subarachnoid hemorrhage (PCT/EP2022/052203). Haptoglobin has been provided free of charge by CSL Behring in the framework of an Innosuisse collaboration with the University of Zurich.

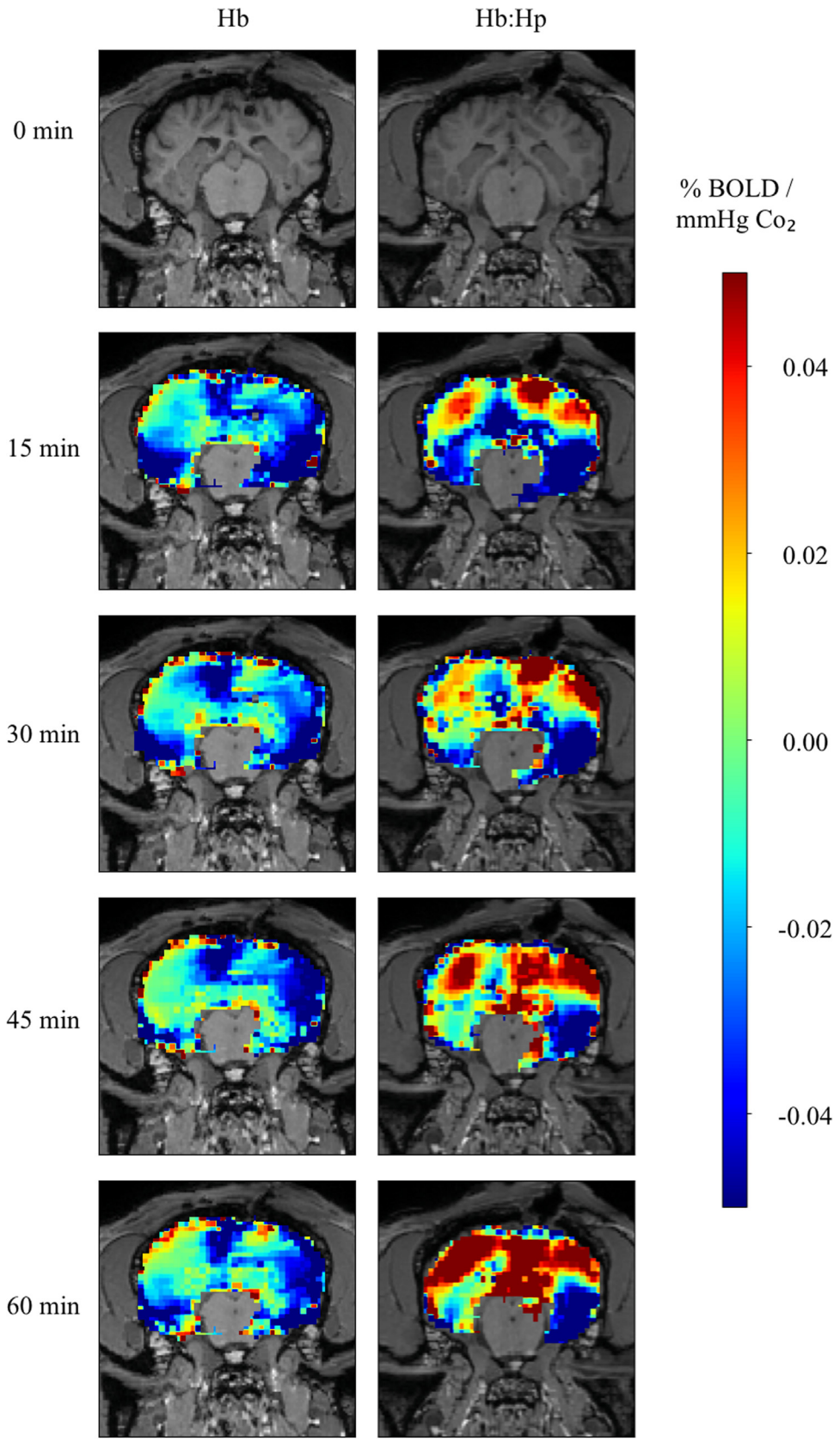

Fig. 3. ***Spatio-temporal dynamics of BOLD-CVR after intracerebroventricular Hb or Hb:Haptoglobin.*** *Spatio-temporal CVR group mean changes after baseline following infusion of 3 mL 3mmol/L Hb (left column) and Hb:Haptoglobin (Hb:Hp, right column) into the CSF space. Colorbar indicates CVR change with respect to baseline.*

CRediT authorship contribution statement

Bart R. Thomson: Methodology, Writing – original draft, Writing – review & editing. **Henning Richter:** Methodology, Writing – review & editing. **Kevin Akeret:** Conceptualization, Methodology, Writing – original draft, Writing – review & editing. **Raphael M. Buzzi:** Conceptualization, Methodology, Funding acquisition, Writing – review & editing. **Vania Anagnostakou:** Methodology, Writing – review & editing. **Christiaan H.B. van Niftrik:** Methodology, Writing – review & editing. **Nina Schwendinger:** Methodology, Writing – review & editing. **Zsolt Kulcsar:** Methodology, Writing – review & editing. **Peter W. Kronen:** Methodology, Writing – review & editing. **Luca Regli:** Project administration, Writing – review & editing. **Jorn Fierstra:** Conceptualization, Methodology, Supervision, Writing – review & editing. **Dominik J. Schaer:** Conceptualization, Methodology, Funding acquisition, Project administration, Supervision, Writing – original draft, Writing – review & editing. **Michael Hugelshofer:** Conceptualization, Methodology, Funding acquisition, Project administration, Supervision, Writing – original draft, Writing – review & editing.

Funding

The work was supported by Innosuisse (grant 19300.1 PF), the Swiss National Science Foundation (grant 310030_197823) and the Uniscientia Foundation (grant 174-2020).

Acknowledgements

Not applicable.

Supplementary materials

Supplementary material associated with this article can be found in the online version at doi:10.1016/j.jstrokecerebrovasdis.2023.106985.

References

1. van Gijn J, Kerr RS, Rinkel GJE. Subarachnoid haemorrhage. Lancet North Am Ed 2007;369:306-318. https://doi.org/10.1016/s0140-6736(07)60153-6.
2. Rincon F, Rossenwasser RH, Dumont A. The epidemiology of admissions of nontraumatic subarachnoid hemorrhage in the United States. Neurosurgery 2013;73:217-223. https://doi.org/10.1227/01.neu.0000430290.93304.33.
3. Sehba FA, Chereshnev I, Maayani S, Friedrich Jr V, Bederson JB. Nitric oxide synthase in acute alteration of nitric oxide levels after subarachnoid hemorrhage. Neurosurgery 2004;55:671-677. discussion 677–8.
4. Dorsch N. A clinical review of cerebral vasospasm and delayed ischaemia following aneurysm rupture. Acta Neurochir Suppl 2011;110:5-6.
5. Akeret K, Buzzi RM, Schaer CA, et al. Cerebrospinal fluid hemoglobin drives subarachnoid hemorrhage-related secondary brain injury. J Cereb Blood Flow Metab 2021:271678X211020629.
6. Hugelshofer M, Sikorski CM, Seule M, et al. Cell-Free oxyhemoglobin in cerebrospinal fluid after aneurysmal subarachnoid hemorrhage: biomarker and potential therapeutic target. World Neurosurg 2018;120:e660-e666. https://doi.org/10.1016/j.wneu.2018.08.141.
7. Deuel JW, Schaer CA, Boretti FS, et al. Hemoglobinuria-related acute kidney injury is driven by intrarenal oxidative reactions triggering a heme toxicity response. Cell Death Dis 2016;7:e2064.
8. Schaer CA, Deuel JW, Schildknecht D, et al. Haptoglobin preserves vascular nitric oxide signaling during hemolysis. Am J Respir Crit Care Med 2016;193:1111-1122.
9. Deuel JW, Vallelian F, Schaer CA, Puglia M, Buehler PW, Schaer DJ. Different target specificities of haptoglobin and hemopexin define a sequential protection system against vascular hemoglobin toxicity. Free Radic Biol Med 2015;89:931-943.
10. Hugelshofer M, Buzzi RM, Schaer CA, et al. Haptoglobin administration into the subarachnoid space prevents hemoglobin-induced cerebral vasospasm. J Clin Invest 2019;129:5219-5235.
11. Garland P, Morton MJ, Haskins W, et al. Haemoglobin causes neuronal damage in vivo which is preventable by haptoglobin. Brain Commun 2020;2:fcz053.
12. Terpolilli NA, Brem C, Bühler D, Plesnila N. Are we barking up the wrong vessels? Cerebral microcirculation after subarachnoid hemorrhage. Stroke 2015;46:3014-3019.
13. Bolar DS, Gagoski B, Orbach DB, et al. Comparison of CBF measured with combined velocity-selective arterial spin-labeling and pulsed arterial spin-labeling to blood flow patterns assessed by conventional angiography in pediatric Moyamoya. AJNR Am J Neuroradiol 2019;40:1842-1849.
14. Mutch WAC, Mandell DM, Fisher JA, et al. Approaches to brain stress testing: BOLD magnetic resonance imaging with computer-controlled delivery of carbon dioxide. PLoS One 2012;7:e47443.
15. Fierstra J, Sobczyk O, Battisti-Charbonney A, et al. Measuring cerebrovascular reactivity: what stimulus to use? J Physiol 2013;591:5809-5821.
16. Elmer J, Harris DR, Sun G, Palmer AF. Purification of hemoglobin by tangential flow filtration with diafiltration. *Biotechnol* Prog 2009;25:1402-1410.
17. Slessarev M, Han J, Mardimae A, et al. Prospective targeting and control of end-tidal CO2 and O2 concentrations. J Physiol 2007;581:1207-1219.
18. Fedorov A, et al. 3D Slicer as an image computing platform for the quantitative imaging network. Magn Reson Imaging 2012;30:1323-1341.
19. Duffin J, et al. The dynamics of cerebrovascular reactivity shown with transfer function analysis. Neuroimage 2015;114:207-216.
20. Cleveland WS. Robust locally weighted regression and smoothing scatterplots. J Am Statist Assoc 1979;74:829-836.
21. van Niftrik CHB, et al. Iterative analysis of cerebrovascular reactivity dynamic response by temporal decomposition. Brain Behav 2017;7:e00705.
22. Iliff JJ, et al. A paravascular pathway facilitates CSF flow through the brain parenchyma and the clearance of interstitial solutes, including amyloid β. Sci Transl Med 2012;4:147ra111.
23. Diringer MN. Controversy: does prevention of vasospasm in subarachnoid hemorrhage improve clinical outcome? Stroke 2013;44:S29-S30.

24. Pickard JD, et al. Effect of oral nimodipine on cerebral infarction and outcome after subarachnoid haemorrhage: British aneurysm nimodipine trial. BMJ 1989;298:636-642.
25. Silvestrini M, et al. Impaired cerebral vasoreactivity and risk of stroke in patients with asymptomatic carotid artery stenosis. JAMA 2000;283:2122-2127.
26. Sasoh M, et al. Effects of EC-IC bypass surgery on cognitive impairment in patients with hemodynamic cerebral ischemia. Surg Neurol 2003;59:455-460. discussion 460−3.
27. Markus H, Cullinane M. Severely impaired cerebrovascular reactivity predicts stroke and TIA risk in patients with carotid artery stenosis and occlusion. Brain 2001;124:457-467.
28. Carrera E, et al. Cerebrovascular carbon dioxide reactivity and delayed cerebral ischemia after subarachnoid hemorrhage. Arch Neurol 2010;67:434-439. **4**.
29. Tancredi FB, Hoge RD. Comparison of cerebral vascular reactivity measures obtained using breath-holding and CO2 inhalation. J Cereb Blood Flow Metab 2013;33:1066-1074.
30. Ogawa S, et al. Functional brain mapping by blood oxygenation level-dependent contrast magnetic resonance imaging. A comparison of signal characteristics with a biophysical model. Biophys J 1993;64:803-812.
31. Sebök M, et al. Mapping Cerebrovascular Reactivity Impairment in Patients With Symptomatic Unilateral Carotid Artery Disease. J Am Heart Assoc 2021;10: e020792.
32. John SE, et al. The ovine motor cortex: A review of functional mapping and cytoarchitecture. Neurosci Biobehav Rev 2017;80:306-315.
33. Artru AA, Momota Y. Rate of CSF Formation and Resistance to Reabsorption of CSF During Sevoflurane or Remifentanil in Rabbits. J Neurosurg Anesthesiol 2000;12:37-43.
34. Munting LP, et al. Influence of different isoflurane anesthesia protocols on murine cerebral hemodynamics measured with pseudo-continuous arterial spin labeling. NMR Biomed 2019;32:8.. e4105.